

Discrepancies between Functional Connectivity measured with BOLD and CBF in Major Depressive Disorder

R. C. Craddock¹, C. B. Glielmi², P. E. Holtzheimer³, X. P. Hu⁴, and H. S. Mayberg⁵

¹ECE, Georgia Tech, Atlanta, GA, United States, ²BME, Georgia Tech and Emory University, Atlanta, Ga, United States, ³Psychiatry, Emory University, Atlanta, Georgia, United States, ⁴BME, Georgia Tech and Emory University, Atlanta, GA, United States, ⁵Psychiatry, Emory University, Atlanta, GA, United States

Introduction

Resting state functional connectivity in fMRI is typically assessed using blood oxygenation level dependent (BOLD) contrast. While BOLD is a well validated marker of neuronal activity, it does not paint a clear picture of the physiological processes involved in that activity, since BOLD is derived from a complex interaction of cerebral blood flow (CBF), cerebral blood volume (CBV) and blood oxygenation (CMRO₂). It is not known whether functional connectivity as measured by correlations in BOLD is driven primarily by correlations in the CMRO₂, CBF, or CBV components of BOLD. Certainly it is possible that the processes mediating functional connectivity vary by location and neural network. We assess the contributions of CBF and BOLD in specific networks associated with major depressive disorder (MDD)^{1,2}. Our objective is to determine if the correlations present in these networks are mediated primarily by CBF or BOLD, and to determine if substructures of these networks behave similarly in both contrasts. Ideally BOLD and CBF would be acquired simultaneously for such a comparison. It is not possible to acquire optimal BOLD and CBF with whole brain coverage in the same PASL acquisition. Instead we acquire the BOLD and CBF resting state data consecutively within the same imaging session.

Methods

34 subjects (24 F, age = 41 +/- 10 years) with MDD participated in accordance with Institutional Review Board Policy. All imaging was performed on a 3T Siemens TIM Trio scanner using a 12 channel head matrix. T1 structural images were acquired in addition to a 7 minute resting state BOLD scan followed by a 7 minute resting state CBF scan. 128 T1 weighted structural images were acquired using a 3D MPRAGE sequence. BOLD data were acquired using a T2* weighted ZSAGA pulse sequence lobe (matrix=64x64, TR=2s, TE=30ms, FA=90°, FOV=220mm, 20 axial slices, voxel resolution 3.4 x 3.4 x 4 mm, 210 measurements) to recover areas affected by susceptibility artifacts³. CBF data were acquired using the pulsed arterial spin labeling FAIR sequence⁴ (matrix=64x64, TR=2.5s, TE=11ms, GRAPPA3, FA=90°, 20 axial slices, voxel resolution 3.4 x 3.4 x 4 mm, labeling time = 700ms, post labeling delay = 1s, 168 measurements). During resting state scans subjects were asked to keep their eyes open, fixate on a point, with no other cognitive instructions (resting awake).

Image preprocessing was performed using the SPM5 toolbox⁵ running in Matlab R14 (Mathworks, Natick, MA). Structural images were simultaneously segmented and normalized to MNI space. Functional scans were slice timing corrected, motion corrected, co-registered to T1, written to MNI space using the transformation matrix calculated for the T1, and spatially smoothed with a 6mm FWHM Gaussian filter. Perfusion data was subtracted (label - control I) after motion correction and prior to co-registration. Functional connectivity analysis was performed on BOLD, and CBF weighted datasets using AFNI⁶ (build 2007_05_29_1644). Seeds were chosen as 6 mm radius spheres located at the center of the subgenual cingulate (sACC25), and the center of the ventral posterior cingulate (vPCC) separate analysis were performed for each seed. Image data were band-pass filtered (0.009 < 0.08). The mean time course was extracted from a seed and used as a regressor of interest along with the global mean time course, and six motion correction time courses as confounders in a general linear model analysis. Resulting fit statistics were converted to correlation coefficients and transformed using the Fisher transformation. Second level analysis was performed using a one sample t-test. In a second analysis of the CBF data, scans were averaged for each subject. These mean values were subtracted for each ROI and correlated across subjects with every voxel of the mean CBF data. This is similar to a typical PET O15 functional connectivity analysis. ROIs for several brain regions were selected from the WFU pickatlas and used to extract mean correlation values for a quantitative comparison.

Results

The resulting functional connectivity maps for sACC25 and vPCC are shown in Figure 1. These CBF images correspond to the mean CBF analysis. The temporal correlation analysis resulted in images that were too noisy to compare. Table 1 contains mean correlation coefficients for several ROIs identified from these maps. In the sACC25 correlation maps (Figure 1 a, b): CBF and BOLD FC maps show similar positive correlations with the thalamus. Discordant correlations are seen with mid cingulate and anterior insula (both strongly negative w/ BOLD, weakly positive w/ CBF). For the vPCC seed (Figure 1 c, d): CBF and PASL FC maps show similar positive correlations of vPCC with thalamus and hypothalamus and similar negative correlations with the anterior and posterior insula, lateral prefrontal, and premotor cortex. Additional correlations are seen only with BOLD: positive correlations of PCC with sACC, medial frontal cortex and hippocampus and negative correlations with mid cingulate. These data are illustrated quantitatively in Table 1. The differences in connectivity between the two contrasts might be explained by neurovascular coupling, the contributions of CBV or inherent error in the measurement and analysis techniques. Or they might point to underlying physiological differences between brain regions/networks. Understanding these FC discrepancies will be the focus of future work.

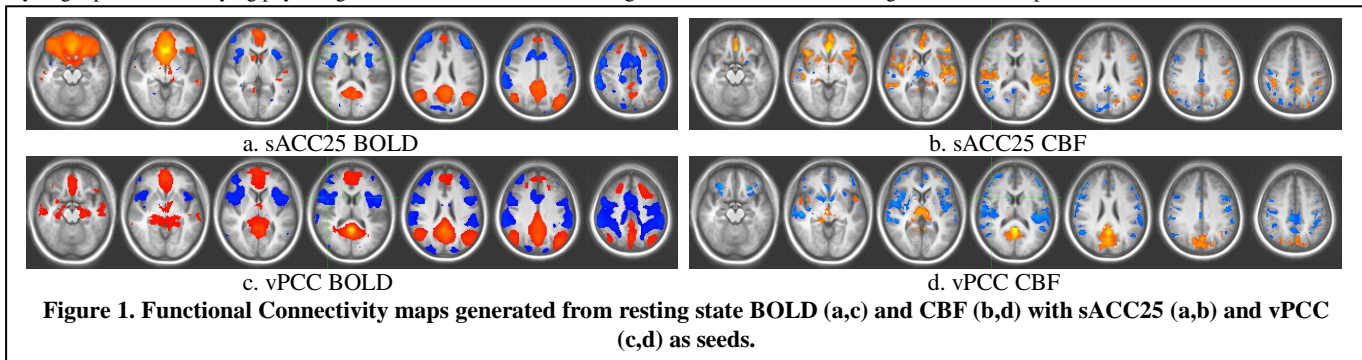


Table 1. Mean Correlation Coefficients in for supra-threshold voxels ($R > .15$) in designated ROIs

	vPCC Seed		CG25 Seed	
	BOLD	CBF	BOLD	CBF
ACC	0.23	-0.25	0.43	0.46
Caudate	0.17	-0.32	0.28	0.26
MF10	-0.21	-0.29	0.10	0.26
Parietal	-0.16	-0.20	-0.16	0.07
Insula	-0.22	-0.30	-0.22	0.37
mF9	0.17	-0.23	0.32	0.35
oF11	-	0.15	0.22	0.22
Hippocampus	0.19	0.19	0.03	0.13
PCC	0.54	0.56	0.25	-0.18
Precuneus	0.22	0.23	0.21	0.01
sACC25	0.20	-0.25	0.32	0.22
lPF9	-0.02	-0.21	0.03	0.27
Thalamus	0.17	0.37	-0.14	-0.17

Ref: 1. Mayberg HS. et al. *Neuron*. 2005; 45(5) 651. 2. Grecius MD. et al. *Biol. Psychiatry*. 2007; 62(5): 429. 3. Heberlein KA, & Hu XP. *MRM* 2004; 51: 212. 4. Wang J et al. *MRM* 2002; 48:242. 7. 5. Friston KJ. *Trends Cogn Sci* 1997; 1:21. 6. Cox RW. *Comput Biomed Res* 1996; 29:162.

Acknowledgements: Funding and salary support from the National Institute of Health P50MH058922 to HSM.